Wet and dry spells in Senegal: Evaluation of satellite-based and model re-analysis rainfall estimates

Cheikh Modou Noreyni Fall[1], Christophe Lavaysse[2], Mamadou Simina Drame[1], Geremy Panthou[2], and Amadou Thierno Gaye[1]

[1]Laboratoire de Physique de l'Atmosphère et de l'Océan—Simeon Fongang, ESP, Univ. Cheikh Anta Diop, Dakar, Senegal
[2]Institut des Géosciences de l'Environnement IGE, Univ. Grenoble Alpes, IRD, CNRS, Grenoble INP, 38000 Grenoble, France

Correspondence: Noreyni Fall (noreyni27@gmail.com)

Abstract. In this study, the detection and characteristics of dry and wet spells (defined as episodes when precipitations are abnormally low or high compared to the climatology) from a large amount of datasets are compared over Senegal. Four datasets are based on satellite data (TRMM-3B42 V7, CMORPH V1.0, TAMSAT V3, CHIRPS V2. 0), two fully based on (re)analyses (NCEP-CFSR, ERA5) and three fully based on raingauge observations (CPC Unified V1.0/RT) and the 65 raingauge network that has been reggrided by using two kriging methods namely Ordinary kriging (OK) and Block kriging (BK). All datasets were converted to same the same spatio-temporal resolution: daily rainfall at $0.25°$. Despite a fairly close agreement between datasets on the seasonal rainfall amounts, the results showed significant disparities in the distribution of dry and wet spells. The occurrence of dry spells is lower in products using Infrared measurement techniques as opposed to products that couple infrared and microwave techniques where these dry spell events are more frequent. All datasets show that dry spells are more frequent at the beginning and end of the rainy season, indicating a false start and early cessation of precipitation. While, the strongest contrasts between the data products are observed on the amplitude of wet sequences. Indeed, these wet strong rainfall events are more intense in OK and TRMM than in the other datasets. Finally, the products are quite similar on the frequency of wet sequences that generally occur during the height of the West African monsoon.

Several studies related to the effect of climate change, predict an intensification of the hydrological cycle, and thus an increased probability of heavy rainfall and dry spells, associated with global warming (Held and Soden, 2008; Giorgi et al., 2011; Trenberth, 2011; Kendon et al., 2019; Berthou et al., 2019). An increase of extreme events is one of the main phenomena accompanying the rainfall recovery in th Sahel (Alhassane et al., 2013; Descroix et al., 2016; Panthou et al., 2014, 2018; Taylor et al., 2017; Wilcox et al., 2018). It is estimated that up to 1.7 million peoples have been affected by floods in Benin, Burkina Faso, Chad, Ghana, Niger, Nigeria and Togo since the second half of the 2000s (Sarr, 2012). In 2009, Benin, Burkina Faso, Niger and Senegal all reported major floods. In 2012, heavy rains affected more than 80% of Nigeria. Extreme events occurred in Burkina Faso, including record rainfall of 263 mm in Ouagadougou during September 2009 (Lafore et al., 2017). In Senegal,

more than 26 peoples died because of direct and indirect impacts of an extreme rainfall event on 26 August 2012 marked by 161 mm in less than 3 hours (Sagna et al., 2015).

On the other hand, in 2012, UN agencies estimated that more than 16 million people in Mali, Sudan, Niger, Burkina Faso, Senegal and Chad were affected by the drought (Program, 2017). In 2014, a severe drought affected several localities in Senegal, leading the Senegalese government to receive US 16.5 million in funding from the African Risk Capacity (ARC, 2014). In addition, according to the World Food Program (WFP), Senegal is one of the seven Sahelian countries where the number of food insecure people will increase significantly from the current 314,600 to 548,000 during the lean season of 2018 (WFP, 2018).

In this context of high risk associated with extreme hydro-meteorological events due to the high vulnerability of the population, it is important to better understand regime and multi-scale rainfall variability (Le Barbé et al., 2002; Lebel and Ali, 2009; Nicholson, 2013; Dione et al., 2014; Yeni and Alpas, 2017). Some studies using raingauges, rainfall estimates from satellite imagery and Numerical Weather Prediction (NWP) have focused on the multi-scales variability of these potentially high-impact events (Washington et al., 2006; Sane et al., 2018; Nicholson et al., 2018). Indeed, since the partial recovery of rainfall, the Sahel observes mixed dry/wet seasonal rainfall features called hybrid rainy seasons (Salack et al., 2016). These hybrid rainy seasons illustrating a rainfall regime intensification is part of what Giorgi et al. (2011) have defined as a more extreme hydrological climate, with longer dry spells and more intense rainfall (Trenberth et al., 2003; Trenberth, 2011). However, a more thorough analysis of the components of these hybrid seasons has not been performed. Although other studies have analyzed the spatial and temporal variability of dry and wet spells over West Africa showing that it is closely related to the spatial and temporal variability of the West African monsoon (Froidurot and Diedhiou, 2017). Moreover, the seasonal cycle of these longer dry spells has higher occurrences at the beginning and end of the rainy season, making them crucial in agro-climatic monitoring (Salack et al., 2013). In Senegal, the studies of Dieng et al. (2008) showed that a long earlier (later) dry spell is associated with higher (lower) seasonal rainfall amounts in July-August-September in the north. In contrast, this relationship is less clear in the south of the country. Understanding and monitoring these high-impact events can produce relevant and important applications in agronomy and in disaster risk management.

Unfortunately, very few studies have compared the performance of satellite imagery, reanalysis products and ground observations on the distribution of dry and wet spells over Sahel. The few comparison studies that have been conducted in Africa have focused mainly on interannual variability of seasonal rainfall amounts (Thorne et al., 2001; Ali et al., 2005). It has been shown that TAMSAT has proven successful in many parts of Africa despite the relative simplicity of its algorithm (Thorne et al., 2001; Jobart et al., 2011; Dinku et al., 2007; Maidment et al., 2013). The CMORPH algorithm shows good agreement with gauge data in Ethiopia but strongly underestimates rainfall amount in the Sahel (Jobard et al., 2010). Moreover, Past studies have also shown that the TRMM 3B42 data can adequately capture the spatial variation in annual and seasonal precipitation (Xu et al., 2019). Nevertheless, it tends to overestimate trace precipitation and underestimate torrential precipitation at the daily scale owing to inadequate detection capability (Xu et al., 2019; Shuhong et al., 2019). Reanalyses are often of poorer quality in the tropics, particularly in Africa where there is unfortunately scarce in situ observations (Parker, 2016). Although,

an improvement has been observed since the emergence of satellite observations, which are thus incorporated into assimilation systems (Parker, 2016).

Thus, it appears a strong need for a broad intercomparison study of these products in a region that is both well documented and has a sufficiently dense network of raingauges. This paper aims to provide an inter-comparison between several datasets based on satellite data (TRMM-3B42 V7, TAMSAT V3, CMORPH V1.0, CHIRPS V2.0), two fully based on (re)analyses (NCEP-CFSR, ERA5), and one fully based on gauge observations (CPC Unified V1.0/RT, provided by ANACIM the National Agency of Civil Aviation and Meteorology, see Table 1) that is spatialized by using two kriging technics. This intercomparison focuses on the ability of these datasets to detect high-impact events of dry and wet spells. Firstly, the spatial distribution of seasonal rainfall accumulation and the seasonal cycle of dry days per month are analyzed. Thereafter, potentially high-impact indicators of dry and wet spells are defined and characterized. The paper is structured as follows. Section 2 describes the data and methodology used in our analysis, while Section 3 presents the main results, as well as the statistical tests conducted to determine whether the observed characteristics could have occurred by chance. Section 4 concludes the paper with a summary of our main findings.

1 Data and Methodological approach

1.1 Raingauges data and kriging methods

Daily rainfall data are provided by the National Meteorological Service of Senegal (ANACIM). In order to avoid any heterogeneity, two levels of quality control have been carried out for an objective control of homogeneity. A manual check of suspicious records was performed, followed by other checks including verification of station locations, identification of repeated data, identification of outliers, comparative tests using neighboring stations and examination of suspicious zero values (i.e. missing data or zero precipitation). The period 1991-2010 is the longest period with the maximum number of reliable stations with sufficient spatial coverage essential to meet the study objectives. Even so, the geographical distribution of this network shows a strong imbalance from west to east. Indeed, the network raingauges shows a higher density in the peanut basin (Central Western Zone of the country) compared to the whole country (See Fig 1). This is largely explained by the high agricultural production of this area where rainfall is a limiting factor in economic activity. Because it is difficult to compare raingauges (point measurement) data with satellite datasets (generally aggregated), raingauge data was gridded into a 25 km $^2 \times$ 25 km^2 data resolution using two different kriging methods namely Ordinary Kriging (OK hereafter) and Block Kriging (BK hereafter). Several studies have shown that kriging is one of the most efficient interpolation methods (Creutin and Obled, 1982; Tabios and Salas, 1985; Goovaerts, 2000). Because different technics exist and there are some inherent uncertainties, two kriging methods were used in this study. OK is used to estimate a value at a point in a region for which a variogram is known, using data in the vicinity of the estimation location (Myers, 1997; Chen et al., 2008; Wei et al., 2009). Thus, the equation 1 gives the value of rain estimated by ordinary kriging.

$$Z^k = \sum_{i=1}^{n} \lambda_i Z_i^o \tag{1}$$

where Z^k and Z^o represent respectively rainfall estimate and obseved raingauge value. λ_i are the weights assigned to the n available observations. Note that, the kriging weights λ_i are derived from an optimization scheme containing $(n+1)$ simultaneous linear equations (Wei et al., 2009). The second kriging technic, BK, is uses a moving neighborhood or block of given dimensions to estimate the average Z value over a surface (Lloyd and Atkinson, 2001; Maidment et al., 2013). The average value of attribute Z over a block V centered a the block mean value is defined in equation 2.

$$Z_v^k = \frac{1}{n}\sum_{i=1}^{n} Z_i^k \tag{2}$$

The block value Z_v^k is a linear average of the n point estimators and has a minimum variance of estimation error (Cressie, 2006; Bilonick, 2012). The root mean square error (RMSE) of kriging is also estimated. This estimate of the error on kriging is crucial in the Sahelian countries where observation networks are often sparsely distributed. Thus, all areas of the country where the number of rainfall stations is not consistent enough are identified and can be possibly masked to avoid bias in the result.

1.2 Satellite and reanalysis and combined datasets

Since the purpose of this study is to compare the monitoring of wet and dry spells among datasets and their uncertainties, an ensemble of 9 different datasets available are used (See Table 1). These datasets are either satellite products, reanalyses or raingauges. TRMM-3B42 V7 and CMORPH V1.0 are exclusively satellite based, while CHIRPS V2.0 and TAMSAT-V3 combine both gauges and reanalyses with satellite data (Kummerow et al., 1998; Nesbitt et al., 2006; Huffman et al., 2007). TRMM-3B42 V7 and CMORPH V1.0 are characterized by combining infrared and microwave measurements while CHIRPS and TAMSAT use exclusively infrared measurement techniques (Funk et al., 2015; Maidment et al., 2017). Infrared measurements are very indirect but have a high spatio-temporal sampling frequency (Kummerow et al., 1998; Ferraro and Li, 2002; Ferraro, 1997). Conversely, microwave methods allow a better estimation of instantaneous precipitation but have a low temporal sampling frequency (Joyce et al., 2004; Zeweldi and Gebremichael, 2009; Xie et al., 2017). Thus, in order to use the benefits of both estimation techniques, the two methods are coupled as in TRMM-3B42 V7 and CMORPH V1.0. In addition, the TRMM satellite is the first satellite with an active radar instrument on board. This allows it to take into account a proxy of the convective cell tops and cloud characteristics (Maranan et al., 2018). Among the datasets, two of them are reanalyses data, namely NCEP-CFSR and ERA5. The NCEP-CFSR is available on the T62 Gaussian grid (Ebert et al., 2007; Saha et al., 2010). While, ERA5 is based on 4D-Var data assimilation using the 41r2 cycle of the Integrated Forecasting System IFS (Malardel et al., 2016). The last dataset is fully based on raingauges observation (CPC Unified V1.0/RT). CPC Unified V1.0/RT use gauge reports from over 30,000 stations from multiple sources including GTS, COOP, and other national and international agencies (Xie et al., 2017).

To realize a reliable comparison and decrease the impact of the resolution of each product, the same spatial and temporal resolutions as the kriging datasets are used. For datasets with a sub-daily temporal resolution, we calculate daily accumulations like raingauge data. The datasets with spatial resolutions lower than $< 0.25°$ are resampled to $< 0.25°$ using bilinear averaging,

whereas those with spatial resolutions coarser than $< 0.25°$ were resampled to $< 0.25°$ using bi-linear interpolation (Beck et al., 2019).

1.3 Methodological approach

Based on daily rainfall data, different dry and wet spells depending on their duration and intensity are computed on each grid point of the common resolution $0.25°$ and over the period of the different data products. Note that these dry and wet spells are the main components of the new hybrid seasons observed in the Sahel since the end of the great droughts during the 80's. Indeed, the distribution of frequency and duration of wet and dry spells depend strongly on the threshold chosen to define a rainy day (Barring et al., 2006). Several authors have used 0.1 mm to define rainy days as this is the usual accuracy of raingauges (Da et al., 2019). Furthermore, Frei et al. (2003) used a threshold of 1.0 mm, as it is more resistant to measurement errors associated with low precipitation and asserted that precipitation below this amount evaporates directly. In this study, a threshold of 1.0 mm is used. This threshold was used by Diallo et al. (2016) and Froidurot and Diedhiou (2017) in the Sahel.

This work is a first step in identifying potential high-impact events. It is therefore important to have a large sample of wet and dry events to perform robust statistics when comparing sources. However, most of the results presented in the study focus on events that have a return period of minimum ten years, so that they could be considered as extremes or strongly abnormal. Moreover, a large number of definitions (depending on the duration of the episodes and their intensities) are used in order to highlight the sensitivity of each datasets and, in the future, their potential impacts. In the following subsections, definitions of methods for detecting dry and wet spells are presented.

1.3.1 Dry Spells

Two criterions are use to define two different types of dry spells. The first one (hereafter DS) is based on the duration of consecutive dry days. These days are detected when the daily precipitation are lower than 1 mm/day (Diallo et al., 2016). This definition is commonly used to define a dry spell in the Sahel and the methodology employed here is similar to the method defined in Salack et al. (2013). Different intensities of DS are defined depending on their durations (DS short, DS medium, DS long, DS extreme long) descripted in Table 2. The second criterion is based on the accumulated precipitation during a specific periods, and are called Dry Spell Cumulative (DSC). Four durations (i.e. intensities) are then defined; DSC5; i.e. five days with less than 5 mm of rainfall; DSC10; i.e. 10 days with less than 10 mm; DSC15; i.e. 15 days with less than 15 mm and DSC20; i.e. 20 days with less then 20 mm (see Table 2). These DSCs can be considered as periods when the rainfall are not sufficient to significantly moisten the soils and therefore do not provide sufficient water for crop yields (Sivakumar, 1992). The results presented in that study focus on the strongest dry spells (DSC10, DSC20, DSl, DSxl). Nevertheless, all the results from the other duration are presented in supplementary materials.

1.3.2 Wet Spells

As well as dry spells, two criterions are used to detect the wet spells and their intensities. The first is based on the duration of intense rainy days (hereafter called WS). Intense rainy days may be defined with different relative intensities that is why four thresholds (90^{th}, 95^{th}, 99^{th}, 99.5^{th} climatological percentiles of the rainy days during all the years and the entire season) are also defined. After calculations of these WS, and because of the synoptic systems associated with rainfall variabilities over Senegal, it appears that duration equal or longer than 2 days are extremely rare, even for the lowest intensities (percentiles). That is why only two durations are defined, one-day duration (e.g. to monitor daily intense rainfall, WS1) and equal or longer than two-day duration (WSM). So for example WSM 99P represents an wet event with at least two consecutive days with each cumulated rainfall greater than the 99^{th} percentile of rainy days.

The second criterions to define wet events is based on percentiles of specific cumulative periods. These periods are defined according to the different synoptic components that drive the rainfall variability over Senegal. Wet spell cumulative (WSC) is defined as specific periods where cumulative rainfall is above the threshold as shown in Table 3). As for dry spell, in this study we have focused on strongest wet spells (WS1 99P, WSM 99P, WSC5 99P, WSC15 99P,) but all the results are presented in supplementary material.

2 Results

2.1 Seasonal rainfall over Senegal

The first inter-comparison done between all the datasets focuses on the seasonal cycle of the rainfall. Fig. 2 shows the climatology of seasonal precipitation over the overlap period (1998-2010) between the datasets. To get a fair comparison between the products, all the datasets are regridded into the same grid and only grids where observed values derived from kriging methods are considered significant (i.e., the root mean square of kriging data less than 0.5), are kept (Lloyd and Atkinson, 2001). The main characteristics of the precipitation in Senegal, driven by the monsoon flow, is a the South-North gradient of cumulated rainfall. There is a good agreement amongst the products in term of spatial variability and cumulated values (from 100 mm in the north to 1,200 mm in the south). The results are especially closed for TRMM-3B42 V7, CHIRPS V2.0, TAMSAT V3 and the two kriged observed precipitation (OK and BK). The reanalyses seem to underestimate the precipitation in the North (ERA5) or in the South (NCEP). Finally our results for CMORPH confirms the findings of Tian et al. (2007) which showed that the regular smoothing of these precipitation resulting from the "morphing" process could have an effect on the intermittency of precipitation. Thus, short-term events such as local convective rainfall occurring between microwave scans will not be accounted for by this procedure.

It is also interesting to notice the differences over the peanut basin (identified in Fig. 1). This region is an important agricultural area of Senegal with 80% of the exportable peanuts and 70% of the total cereal crop, (Thuo et al., 2014). Because of this importance, a robust network of raingauges (about 24) was used to get a more robust and slightly more complexe structure

of the cumulated rainfall from OK and BK. When looking over smaller areas, differences are more important and any of the products is able to get this structure, even if their bias stay low.

It is also important to notice the large impact of the kriging techniques with the differences between OK and BK because of their calculations (see equation 1 and 2). Indeed, the ordinary kriging assumes stationarity (i.e. the mean and variance of the values are constant in the spatial field) while block kriging estimates mean values over the block rather than over points (Chen et al., 2008; Wei et al., 2009). Thus, maps of the cumulated rainfall using BK is smoother than OK. It means also that BK should be more adapted to be compared to satellite estimation than OK.

So, using BK as reference, it is interesting to note that TRMM is the closest to BK in intensity but only CMORPH is able to reproduce the specific South-East – North-West gradient observed over the Peanut basin. This proximity between TRMM, CMORPH and BK could be explained by the precipitation radar (PR) on board on TRMM or the combination of the infrared and microwave measurements used in CMORPH which seem to be adapted over this region. Maranan et al. (2018) show that these instruments have a better estimation of precipitation by assessing water vapor, cloud water and precipitation intensity in the atmosphere (Maranan et al., 2018).

In addition to the cumulated rainfall, the seasonal evolution of the dry days is crucial. It allows definition of the beginning and the end of the rainy season and the periods of drought. During the dry season (November to May), all datasets agree to record more than 85% of dry days, showing a very low occurrence of off-season rainfall called "Heug" rainfall (Seck, 1962; Gaye et al., 1994). Note that, at the same time, OK and BK record 100% of the dry days possibly due to technical issues and/or absence of data collection during that period. Due to the absence of observed precipitation, it is difficult to know what is the most accurate products, nevertheless, it seems that products such as CMORPH, during all the dry season, and TAMSAT and NCEP for the dry season from October to December overestimate the "Heug" rainfalls. The reasons could be due to the algorithm of CMORPH, that tends to overestimate the small precipitation (Bruster-Flores et al., 2019), which would explain why the differences appear here but not when looking at the cumulated rainfall (Fig. 1). TAMSAT generates too much precipitation days in the southern part of the region. It is also visible in term of cumulated rainfall.

During the rainy season (from June to October), where the occurrence of these dry days is more crucial for socio-economic activity, the differences between datasets increase. The datasets can be decomposed in two groups,TRMM, CPC, NCEP that depict an evolution relatively close to the OK and with all along the season more dry days than the second group (TAMSAT, CHIRPS, CMORPH). The later is closer to the evolution of the BK. Finaly ERA5 is the only products that is similar to OK during the beginning and the end of the season and BK during the central part of it.

It is a difficult to find the reasons of the presence of these two groups. CHIRPS and TAMSAT, which combine in-situ stations with infrared sensors, generally record fewer dry days. It is well known that infrared sensors have difficulties to assess the ground precipitation from cloud top temperature (Ringard, 2017). Another commonality of the two groups is the native resolution of the products. Indeed, even if they are all regridded into the same resolution, TAMSAT, CHIRPS and CMORPH have the highest resolutions (0.0375, 0.05 and $0.05°$ respectively) compare to TRMM, CPC and NCEP (0.25, 0.5 and $0.31°$ respectively, see Table 1). But, this result is counterintuitive since the data with the coarse resolutions are closer to OK, which

is known to be a point interpolation. It is a very surprising result to get the largest percentage of dry days with the coarsest datasets.

Thus, the seasonal cycle of dry days allows us to highlight the complexity of the intermittent rainfall in the datasets and so the potential difficulty to monitor the dry and wet spells. Following this seasonal analysis, the specific comparison of the dry and wet spells detection is done.

2.2 Dry Spells

The purpose of this section is to compare the detection of different type of dry spells (depending their intensity and duration) derived from the 9 products. In the main document, we will focus on the four more sensitive dry spell indicators for the agriculture and livestock, namely DSC10, DSC20, DSl, DSxl (see Table 2 for the definitions). Nevertheless, the same results for the other type of dry spells are presented in supplementary materials. The first comparison done is the average occurrence of dry spells per year (Fig. 4). These occurrences are calculated for all datasets only over grid points where the kriging method is considered significant. The results highlight a good agreement between TAMSAT and CHIRPS on the one hand and CMORPH and TRMM on the other. This is in agreement with the previous results on the dry days (Fig. 4). This result confirms the high sensitivity to the detection of dry spells according to the methods used to extract precipitation datasets. Indeed, TRMM, based on coupling infrared (IR) and microwave (MO), gets more frequent rainfall breaks than TAMSAT and CHIRPS, based on infrared. But, surprisingly, CMORPH, which provides a similar reduced occurrence of dry days than TAMSAT and CHIRPS, produces a comparable occurrence of dry spells to the driest products. This is especially true for the DSl and DSxl. TRMM and CMORPH benefit from the advantages of both IR and MO methods. The principle of IR is based on the proxy of rainfall rate from to top cloud temperature. According to Dinku et al. (2018), IR sensors can overestimate the rainfall rate by considering cirrus clouds as convective clouds. The use of microwave (MO) measurement is a more physical measure of the water content of clouds and provides a better instantaneous estimate of precipitation (Ringard, 2017). This can explained the relative good assessment of the two products compared to the observations, but not the discrepancies of CMORPH between the detection of dry days and the occurrence of dry spells.

To better understand these different behaviors, the seasonal evolution is taken into account (Fig. 5) illustrating the feature of the seasonal evolution of the dry spells over Senegal. Note that, due to their definitions, DSC10, DSC20 and DSxl are very sensitive to the dry season (from November to May), whereas DSl focuses on a specific dry spell duration and is more sensitive during transitional periods (i.e. onset and retreat phase of the rainfall). Hence, there is a coherent grouping of datasets during the rainy season of DSC10 and DSC20 relatively close to those obtained with the frequency of dry days in Fig. 3. A significant result is the delay of the rainy season generated by the two reanalyses. Indeed, ERA5 and NCEP reveal an overestimation of the DSC10, DSC20 and DSxl during the period from May to July. The established and retreat phases of the monsoon are much better in agreement with the observations. The evolution of DSl is also interesting by focusing on relative mild droughts with specific durations that are sensitive to dry spells during the onset and retreat phases of the monsoon. This detection is, by far, the more variable from one product to another. For this specific drought it is difficult to distinguish specific behavior of a group of products. Each possesses a specific time evolution with a larger peak either during the onset (June) or the retreat phase

(September). Some delays are also visible during the retreat phase (TAMSAT for instance). Finally, it is remarkable to see the very good agreement between OK and CPC. According to this Fig. 5 two conclusions could be drawn, first is the complexity to monitor the seasonal evolution of specific dry spells over Senegal despite a good agreement at the wider scale. The second is the difficulty to consider the reference. Indeed, even when using observations, the necessity to spatialize the data by using kriging methods reveals very large impact in term of dry spell detection.

In order to synthesize the agreement amongst the datasets on the spatial variability of the different dry spells the Taylor diagram (Taylor, 2001) is plotted (Fig. 6). This type of graphic gives a large overview of the capacity of datasets to agree on the spatial distribution by providing simultaneously three pieces of information: the spatial correlation, the standard deviation, and the root mean square deviation (RMSD) compared to a reference. Here, the reference is defined as BK. This is motivated by the fact that this kriging method, with a spatial assessment over grid boxes is more relevant to be compared against the spatial datasets. The same results compared to OK are providing in supplementary materials. Not surprisingly, DSC20 and DSxl are more stable and so display the lowest values of standard deviation. For the DSC10 and DSC20 and the DSl there is no clear difference amongst the datasets. However, DSC10 is more sensitive to the datasets. Overall, TRMM looks to be the closest and so the best product to detect these dry spells. TAMSAT and CHIRPS also display a good score with a correlation larger than 0.85, a standard deviation of 1 and a RMSD close to 0.5. By contrast, CPC records the lowest scores. It is also worth noting that the methodology of generating the kriging of observation datasets generates a big difference. Hence, OK is generally one of the largest RMSD and lowest correlation scores. It is important to notice that the differences among the products are comparable to the uncertainties related to the kriging methods of observations.

Finally, Fig. 7 depicts the comparison of the interannual variability of occurrence of dry spells. The figures reveals the big challenge of assessing the climatological trends due to the large inter-annual variability of these events, the discrepancies between datasets, and sometimes the opposite temporal evolutions. Overall, DSC10 and DSC20 display a slight decrease of events. This is observed by all the products except CPC and ERA5. DSxl displays some similitude to this climatological evolution. Nevertheless, the interannual variability is much higher and there is no significant trend detected. Finally, DSl displays a specific time evolution. It is worth to note that, except the biases, the time evolutions of all the products are in good agreement, displaying an increase of these DSl during the beginning of the 2000's with a peak in 2003-2004. It is also worth noting that, even if the spatial coherences of the two kriging technics are low, their interannual evolutions are close.

2.3 Wet Spells

In this section, the same work on intercomparison of the datasets to monitor wet spells (depending on their intensity and duration) is assessed. In the main document, four types of wet spells using the 99th percentile of rain amount per day are used as thresholds, namely WS1 99P, WSM 99P, WSC5 99P, WSC15 99P (see Table 3) are discussed. The results using the other definitions of wet spells are presented in supplementary material. Regarding the intensity of events detected (Fig. 8), there are two main findings. First TRMM appears to be significantly better, and closer to the observations, than the other products. This is true for all the wet spell definitions. All the other products clearly underestimate the events, especially when looking at OK.

Regarding BK, which is, by definition, associated with smoother datasets, the differences are smaller, but still exist especially for the WSCs (bottom panels in Fig. 8).

The seasonal cycles of wet spells with short durations (WS1 99P and WSC5 99P, Fig. 9) agree amongst the products. The only significant differences are found with the underestimation of CHIRPS, CPC and TAMSAT and the delay of CMORPH to represent the peak during the hearth of the rainy season. For the WSC15, the same distribution is found and the differences (in term of intensity or timing) are not significant. Finally, WSM 99P, which is one of the most intense events, displays more variability. It is worth noting that CHIRPS underestimated the WSI 99P and has the most frequent WSM 99P. The reasons are not well understood.

In order to better explain the reasons for these differences, the logarithmic distribution of daily rainfall over the common period (from 1998 to 2010) is calculated (Fig. 10). This distribution shows to see tipping points on daily rainfall. Daily rainfall less than 25mm are more frequent on TAMSAT and CHIRPS. These two products record the most rainy days in the main season (Fig. 2). But the decrease toward more intense daily rainfall is more abrupt than the others products. This results in the lowest number of high daily rainfall for TAMSAT, with a maximum at about 50 mm. CHIRPS and CMORPH are also associated with a slight underestimations of strong daily rainfall (no event beyond 90mm). By contrast, TRMM produces the largest rainfall events. This anomaly starts for mild events (around 30mm) to the most extreme cases (larger than 120 mm).

The Taylor diagram, to assess the spatial variability of the wet spells (Fig. 11), presents much more variability than for the dry spells (Fig. 6). As for the previous diagram, the reference is still defined as BK, but the results using OK are provided in supplementary materials. These results show globally lower score for WS than DS resulting from the scarcity and then variability of these events. Moreover the difference in between products is much more pronounced highlighting the uncertainties of monitoring WS. It is also worth noting that cumulative scores (WSCs) obtain better scores. As shown in the previous figures, TRMM appears to be the closest to the observations, except to the WSM 99P. This could be explained by the very strict criterions to detect them and the fact that only a few cases were recorded during the common period. Surprisingly, despite large discrepancies in the distribution of the daily rainfall (Fig. 10), TAMSAT is relatively good at representing the variability of these events. The fact that our criterions are using quantiles instead of specific amount of rainfall contributes bias correction of this underestimation. By contrast, CMORPH is generally the farthest to BK pointing out the difficulties to represent the spatial variability of the occurrences of these events.

Finally, the recent climatological trend and the interannual variability of these extreme events (Fig. 12) show a large interannual variability and, as for the dry spells, large differences amongst the products. The temporal correlations are, for most of the products, not significant when compared to OK or BK. Recently, for almost all the products and wet spells, there is an increase of occurrence, especially for WSC5 99P and WSC15 99P. For the two products based on observations, the temperal evolution are very close and display a major increase in all the indicators. That may be in line with the recent study of Taylor et al. (2017) suggesting that the Mesoscale Convective Systems (MCSs) responsible for extreme rainfall in the Sahel increased recently. Nevertheless, this could be also related to a strong abnormal year of 2010.

2.4 Discussions

In this study, comparisons between a wide variety of data sets are made to assess the uncertainties in monitoring wet and dry periods in Senegal. Significant differences and uncertainties are observed. The product resulting from the observations and kriged with the BK method is identified as the reference. This is justified by the fact that kriged data are more likely to be compared with satellite observations or model data. This method, representing mean precipitation over a grid, is also more comparable to the integrated data of the other products. To improve our understanding, once the results of these comparisons were obtained, some explanations for these relatively good or bad scores are conducted. The first investigation focuses on the resolution of the products. Even if all the products are regrided on identical grids, the original resolution of the products is very different from one product to another. However, the results obtained are counter-intuitive. Especially for dry spells, with more dry spells coming from the finest products. For wet periods, it turns out that the products with the lowest intense rainfall are also the finest. This explanation is therefore probably not sufficient. Satellite products combining infrared and microwaves allow good sampling (IR) with better intensity extractions (MO). TRMM and CMORPH using this combination show similar trends and are often quite close to in situ observations (OK and BK). Moreover, the proximity between TRMM and raingauges (OK and BK) still seems to highlight the contribution of the radar on board the TRMM satellite. It should be recalled that TRMM is the first satellite equipped with an active radar instrument on board. This is indeed a strong added value since it provides a profile of rainfall activity. It is also important because the data obtained show the structure of precipitation in clouds, the type and vertical extent of this precipitation and the freezing point height by determining the level of the bright band. As far as the reanalyses (ERA5 and NCEP) are concerned, they very quickly show their limitations in reproducing these precipitation events. It is important to note that precipitation is generally not a reanalysis product but is derived from short-term forecasts in the reanalysis cycle. Observations are thus not assimilated and the products are generally presented as less robust from the providers. Overall, the results confirm the conclusions of Siegmund et al. (2015) on reanalyses. Indeed, in unimodal regions such as the Sahel, the reanalyses are quite close on the main characteristics of the seasonal rainfall cycle and seasonal evolution. However, they often show quite significant differences in the characteristics of intra-seasonal rainfall.

3 Conclusions

In this study, the monitoring of high potential impact events over Senegal are compared using from 4 satellite products (TRMM-3B42 V7, CMORPH V1.0, CHIRPS V2.0, TAMSAT V3), 2 reanalysis models (NCEP-CFSR, ERA5) and 3 products on raingauges (CPC Unified V1.0/RT, OK, BK). To do so, the same spatial resolution is used for all the products by upgrading or kriging technics to get the same the spatial resolution of $0.25° \times 0.25°$.

Large scale climatology of seasonal rainfall shows fair agreement between the products, particularly on the well known South-North gradient of rainfall associated with the West African monsoon. However, some differences in the magnitude of seasonal rainfall amounts are observed. when looking over specific regions. TRMM, TAMSAT, CHIRPS provide seasonal cumulated rainfall very close to BK. This specific kriging technique is defined as the reference because the estimation is done for an average rainfall over pixels like most of the satellite products. Nevertheless, this good agreement amongst the products

start to dissipate when analyzing the seasonal cycle of dry days. Two groups of data appeared, one recording more dry days than the other. It turned out that each of the kriging methods were positioned in these groups. The impact of the spatial resolution was thus hypothesized. Indeed, OK is reduced to a point while BK estimates average values on grid "blocks" rather than individual points. However, it turns out that this hypothesis was not confirmed.

The study then focused on the monitoring of dry spells indicators. Two types of dry spells are tested. The first (DS) is based on the duration of dry days (precipitation lower than 1 mm). The second (DSC) is a minimum of rainfall per specific durations (for exemple, DSC10 for 10-d cumulated precipitation lower than 10mm). It turns out that TAMSAT and CHIRPS, using infrared-based methods, obtain low occurrences of DS and DSC. On the other hand, CMORPH and TRMM, using methods coupling infrared (IR) and microwave (MO), have more DS.

However, there is less agreement between the different data products for dry spells than for the wet spells. Indeed, the scores are more distant from the reference, BK. TRMM is particularly accurate and close to observations, and the intensity of wet events in TRMM and BK can sometimes be more than double that of TAMSAT and CHIRPS, which underestimate the intensity of these events. CMORPH and reanalyses provide fairly moderate intensities. The trend that has emerged is that satellite products that combine raingauges record the rainiest days but minimize these high rainfall events. In addition, the proximity between TRMM and BK can be explained by the radar on board the TRMM satellite. Because even though CMORPH combines infrared and microwave sensors like TRMM, it is not as close to OK or BK as TRMM. Thus, only the radar seems to favour TRMM's performance.

Finally, the climatologic trends and inter-annual evolutions are tested. There is a slight trend towards a decrease of the DS for the products and a positive but not significant trend of the WS. The too short duration for all the products that are available may explain this insignificance.

This study shows that despite the general agreement on seasonal precipitation, there is a large uncertainty associated with the monitoring of extreme wet and dry spells at the intra-seasonal time scale. This study allows validating the most robust datasets, TRMM, for Senegal that could potentially be extrapolated to the whole of West Africa. This is crucial for monitoring, forecasting and determining the potential socio-economic impact of these periods of extreme drought and humidity.

Author contributions. NF made the analysis and, NF, CL, MD GP discuss the results and wrote the paper. GP supports this study for the kriging methods. AG advises and provides scientific recommendations

Competing interests. The authors declare that they have no conflict of interest.

References

Alhassane, A., Salack, S., Ly, M., Lona, I., Traore, S., and Sarr, B.: Evolution of agro-climatic risks related to the recent trends of the rainfall regime over the Sudano-Sahelian region of West Africa, Science et changements planétaires / Sécheresse, 24, 282–93, https://doi.org/10.1684/sec.2013.0400, 2013.

Ali, A., Amani, A., Diedhiou, A., and Lebel, T.: Rainfall Estimation in the Sahel. Part II: Evaluation of Rain Gauge Networks in the CILSS Countries and Objective Intercomparison of Rainfall Products, Journal of Applied Meteorology - J APPL METEOROL, 44, 1707–1722, https://doi.org/10.1175/JAM2305.1, 2005.

ARC: Risk Pool I – 2014/2015, http://www.africanriskcapacity.org/2016/10/30/risk-pool-i/, 2014.

Barring, L., Holt, T., Linderson, M.-L., Radziejewski, M., Moriondo, M., and Palutikof, J.: Defining dry wet spells for point observations, observed area averages, and regional climate model gridboxes in Europe, Climate Research, 31, 35, https://doi.org/10.3354/cr031035, 2006.

Beck, H., Pan, M., Roy, T., Weedon, G., Pappenberger, F., van Dijk, A., Huffman, G., F. Adler, R., and Wood, E.: Daily evaluation of 26 precipitation datasets using Stage-IV gauge-radar data for the CONUS, Hydrology and Earth System Sciences, 23, 207–224, https://doi.org/10.5194/hess-23-207-2019, 2019.

Berthou, S., Rowell, D. P., Kendon, E. J., Roberts, M. J., Stratton, R. A., Crook, J. A., and Wilcox, C.: Improved climatological precipitation characteristics over West Africa at convection-permitting scales, Climate Dynamics, https://doi.org/10.1007/s00382-019-04759-4, 2019.

Bilonick, R.: An Introduction to Applied Geostatistics, Technometrics, 33, 483–485, https://doi.org/10.1080/00401706.1991.10484886, 2012.

Bruster-Flores, J. L., Ortiz-Gómez, R., Ferriño-Fierro, A. L., Guerra-Cobián, V. H., Burgos-Flores, D., and Lizárraga-Mendiola, L. G.: Evaluation of Precipitation Estimates CMORPH-CRT on Regions of Mexico with Different Climates, Water, 11, https://doi.org/10.3390/w11081722, https://www.mdpi.com/2073-4441/11/8/1722, 2019.

Chen, Y.-C., Wei, C., and Yeh, H.-C.: Rainfall network design using kriging and entropy, Hydrological Processes, 22, 340 – 346, https://doi.org/10.1002/hyp.6292, 2008.

Cressie, N.: Block Kriging for Lognormal Spatial Processes, Mathematical Geology, 38, 413–443, https://doi.org/10.1007/s11004-005-9022-8, 2006.

Creutin, J. and Obled, C.: Objective Analyses and Mapping Techniques for Rainfall Fields: An Objective Comparison, Water Resources Research - WATER RESOUR RES, 18, 413–431, https://doi.org/10.1029/WR018i002p00413, 1982.

Da, J., Jale, S., Fernando, S., Junior, S. F., Fialho, E., Xavier, M., Stosic, T., Stosic, B., Alessandro, T., and Ferreira, E.: Application of Markov chain on daily rainfall data in Paraíba-Brazil from 1995-2015, Acta Scientiarum Technology, 41, 1–10, https://doi.org/10.4025/actascitechnol.v41i1.37186, 2019.

Descroix, L., Diongue Niang, A., Panthou, G., Bodian, A., Sane, Y., Dacosta, H., Malam Abdou, M., Vandervaere, J.-P., and Quantin, G.: Évolution récente de la pluviométrie en Afrique de l'ouest à travers deux régions : la Sénégambie et le Bassin du Niger Moyen, Climatologie, 12, 25–43, https://doi.org/10.4267/climatologie.1105, 2016.

Diallo, I., Giorgi, F., Deme, A., Tall, M., Mariotti, L., and Gaye, A.: Projected changes of summer monsoon extremes and hydroclimatic regimes over West Africa for the twenty-first century, Climate Dynamics, 47, https://doi.org/10.1007/s00382-016-3052-4, 2016.

Dieng, O., Roucou, P., and Louvet, S.: Variabilité intra-saisonnière des précipitations au Sénégal (1951-1996), 2008.

Dinku, T., Ceccato, P., Grover-Kopec, E., Lemma, M., Connor, S. J., and Ropelewski, C. F.: Validation of satellite rainfall products over East Africa's complex topography, International Journal of Remote Sensing, 28, 1503–1526, https://doi.org/10.1080/01431160600954688, https://doi.org/10.1080/01431160600954688, 2007.

Dinku, T., Funk, C., Peterson, P., Maidment, R., Tadesse, T., Gadain, H., and Ceccato, P.: Validation of the CHIRPS Satellite Rainfall Estimates over Eastern of Africa: Validation of the CHIRPS Satellite Rainfall Estimates, Quarterly Journal of the Royal Meteorological Society, https://doi.org/10.1002/qj.3244, 2018.

Dione, C., Lothon, M., Daouda, B., Campistron, B., Couvreux, F., Guichard, F., and Sall, S. M.: Phenomenology of Sahelian convection observed in Niamey during the early monsoon, Quarterly Journal of the Royal Meteorological Society, 140, https://doi.org/10.1002/qj.2149, 2014.

Ebert, E., Janowiak, J., and Kidd, C.: Comparison of Near-Real-Time Precipitation Estimates From Satellite Observations, Bulletin of The American Meteorological Society - BULL AMER METEOROL SOC, 88, https://doi.org/10.1175/BAMS-88-1-47, 2007.

Ferraro, R.: SSM/I derived global rainfall estimates for climatological applications, Journal of Geophysical Research, 1021, 16 715–16 736, https://doi.org/10.1029/97JD01210, 1997.

Ferraro, R. and Li, Q.: Detailed analysis of the error associated with the rainfall retrieved by the NOAA/NESDIS Special Sensor Microwave/Imager algorithm 2. Rainfall over land, Journal of Geophysical Research, 107, https://doi.org/10.1029/2001JD001172, 2002.

Frei, C., Christensen, J., Deque, M., Jacob, D., Jones, R., and Vidale, P.: Daily precipitation statistics in regional climate models: Evaluation and intercomparison for the European Alps, Journal of Geophysical Research, 108, https://doi.org/10.1029/2002JD002287, 2003.

Froidurot, S. and Diedhiou, A.: Characteristics of Wet and Dry Spells in the West African Monsoon System, Atmospheric Science Letters, 18, https://doi.org/10.1002/asl.734, 2017.

Funk, C., Peterson, P., Landsfeld, M., Pedreros, D., Verdin, J., Shukla, S., Husak, G., Rowland, J., Harrison, L., Hoell, A., and Michaelsen, J.: The climate hazards infrared precipitation with stations - A new environmental record for monitoring extremes, Scientific Data, 2, 150 066, https://doi.org/10.1038/sdata.2015.66, 2015.

Gaye, A. T., Fongang, S., Garba, A., and Badiane, D.: Etude des pluies de Heug sur le Senegal a l'aide de donnees conventionnelles et imagerie Meteosat = Study of Heug rainfall in Senegal using conventional data and Meteosat imagery, Veille Climatique Satellitaire, pp. 61–71, http://www.documentation.ird.fr/hor/fdi:41383, 1994.

Giorgi, F., Im, E.-S., Coppola, E., Diffenbaugh, N. S., Gao, X. J., Mariotti, L., and Shi, Y.: Higher Hydroclimatic Intensity with Global Warming, Journal of Climate, 24, 5309–5324, https://doi.org/10.1175/2011JCLI3979.1, 2011.

Goovaerts, P.: Geostatistical Approaches for Incorporating Elevation Into the Spatial Interpolation of Rainfall, Journal of Hydrology, 228, 113–129, https://doi.org/10.1007/s00703-005-0116-0, 2000.

Held, I. M. and Soden, B.: Robust Response of the Hydrological Cycle to Global Warming, AGU Fall Meeting Abstracts, 19, https://doi.org/10.1175/JCLI3990.1, 2008.

Huffman, G., Adler, R., Bolvin, D., Gu, G., Nelkin, E., Bowman, K., Stocker, E., and Wolff, D.: The TRMM multi-satellite precipitation analysis: Quasi-global, multi-year, combined-sensor precipitation estimates at fine scale, J. Hydrometeor., 8, 28–55, 2007.

Jobard, I., Berges, J., Chopin, F., and Roca, R.: EPSAT-SG: A satellite method for precipitation estimation; its concepts and implementation for the AMMA experiment, Annales Geophysicae, 28, 289–308, 2010.

Jobart, I., Chopin, F., Berges, J., and Roca, R.: An intercomparison of 10 days satellite products during West African Monsoon, 2011.

Joyce, R., Janowiak, J., Arkin, P., and Xie, P.: CMORPH: A Method That Produces Global Precipitation Estimates From Passive Microwave and Infrared Data at High Spatial and Temporal Resolution, Journal of Hydrometeorology - J HYDROMETEOROL, 5, https://doi.org/10.1175/1525-7541(2004)005<0487:CAMTPG>2.0.CO;2, 2004.

Kendon, E. J., Stratton, R. A., Marsham, J. H., Berthou, S., and Rowell, David P.and Senior, C. A.: Enhanced future changes in wet and dry extremes over Africa at convection-permitting scale, Nature Communications, 10, 2041–1723, https://doi.org/https://doi.org/10.1038/s41467-019-09776-9, 2019.

Kummerow, C., Barnes, W., Kozu, T., Shiue, J., and Simpson, J.: The Tropical Rainfall Measuring Mission (TRMM) sensor package, Journal of Atmospheric and Oceanic Technology - J ATMOS OCEAN TECHNOL, 15, 809–817, https://doi.org/10.1175/1520-0426(1998)015<0809:TTRMMT>2.0.CO;2, 1998.

Lafore, J.-P., Beucher, F., Peyrillé, P., Diongue-Niang, A., Chapelon, N., Bouniol, D., Caniaux, G., Favot, F., Ferry, F., Guichard, F., Poan, D., Roehrig, R., and Vischel, T.: A multi-scale analysis of the extreme rain event of Ouagadougou in 2009, Quarterly Journal of the Royal Meteorological Society, https://doi.org/10.1002/qj.3165, 2017.

Le Barbé, L., Lebel, T., and Tapsoba, D.: Rainfall Variability in West Africa during the Years 1950–90, Journal of Climate, 15, 187–202, https://doi.org/10.1175/1520-0442(2002)015<0187:RVIWAD>2.0.CO;2, 2002.

Lebel, T. and Ali, A.: Recent trends in the Central and Western Sahel rainfall regime (1990–2007), Journal of Hydrology, 375, 52–64, https://doi.org/10.1016/j.jhydrol.2008.11.030, 2009.

Lloyd, C. and Atkinson, P.: Assessing Uncertainty in Estimates with Ordinary and Indicator Kriging, Computers and Geosciences - COMPUT GEOSCI, 27, 929–937, https://doi.org/10.1016/S0098-3004(00)00132-1, 2001.

Maidment, R., Grimes, D., Allan, R., Greatrex, H., Rojas, O., and Leo, O.: Evaluation of satellite-based and model re-analysis rainfall estimates for Uganda, Meteorological Applications, 20, https://doi.org/10.1002/met.1283, 2013.

Maidment, R., Grimes, D., Black, E., Tarnavsky, E., Young, M., Greatrex, H., Allan, R., Stein, T., Nkonde, E., Senkunda, S., and Uribe, E.: A new, long-term daily satellite-based rainfall dataset for operational monitoring in Africa, Scientific Data, 4, https://doi.org/10.1038/sdata.2017.63, 2017.

Malardel, S., Wedi, N., Deconinck, W., Diamantakis, M., Kühnlein, C., Mozdzynski, G., Hamrud, M., and Smolarkiewicz, P.: A new grid for the IFS, ECMWF Newsletter, 146, 23–28, 2016.

Maranan, M., Fink, A., and Knippertz, P.: Rainfall types over southern West Africa: Objective identification, climatology and synoptic environment, Quarterly Journal of the Royal Meteorological Society, https://doi.org/10.1002/qj.3345, 2018.

Myers, D.: Multivariate geostatistics By Hans Wackernagel, Mathematical Geology, 29, 307–310, https://doi.org/10.1007/BF02769635, 1997.

Nesbitt, S. W., Cifelli, R., and Rutledge, S. A.: Storm Morphology and Rainfall Characteristics of TRMM Precipitation Features, Monthly Weather Review, 134, 2702–2721, https://doi.org/10.1175/MWR3200.1, 2006.

Nicholson, S.: The West African Sahel: A Review of Recent Studies on the Rainfall Regime and Its Interannual Variability, ISRN Meteorology, 2013, https://doi.org/10.1155/2013/453521, 2013.

Nicholson, S., Fink, A., and Funk, C.: Assessing recovery and change in West Africa's rainfall regime from a 161-year record, International Journal of Climatology, 38, 3770–3786, https://doi.org/10.1002/joc.5530, 2018.

Panthou, G., Vischel, T., and Lebel, T.: Recent trends in the regime of extreme rainfall in the Central Sahel, International Journal of Climatology, 34, https://doi.org/10.1002/joc.3984, 2014.

Panthou, G., Lebel, T., Vischel, T., Quantin, G., Sane, Y., Abdramane, B., Ndiaye, O., Diongue Niang, A., and Diopkane, M.: Rainfall intensification in tropical semi-arid regions: The Sahelian case, Environmental Research Letters, 13, https://doi.org/10.1088/1748-9326/aac334, 2018.

Parker, W.: Reanalyses and Observations: What's the Difference?, Bulletin of the American Meteorological Society, 97, 160128144638 003, https://doi.org/10.1175/BAMS-D-14-00226.1, 2016.

Program, U. C. D.: UCDP Conflict Encyclopedia. Uppsala University. www.ucdp.uu.se., 2017.

Ringard, J.: Estimation des précipitations sur le plateau des Guyanes par l'apport de la télédétection satellite, 2017.

Sagna, P., Ndiaye, O., Diop, C., Diongue-Niang, A., and Corneille, S.: Are recent climate variations observed in Senegal in conformity with the descriptions given by the IPCC scenarios?, Atmospheric Pollution, 227, 2015.

Saha, S., Moorthi, S., Pan, H.-L., Wu, X., Wang, J., Nadiga, S., Tripp, P., Kistler, R., Woollen, J., Behringer, D., Liu, H., Stokes, D., Grumbine, R., Gayno, G., Wang, J., Hou, Y.-T., Chuang, H.-Y., Juang, H.-M., Sela, J., and Goldberg, M.: The NCEP climate forecast system reanalysis, Bulletin of The American Meteorological Society - BULL AMER METEOROL SOC, 91, https://doi.org/10.1175/2010BAMS3001.1, 2010.

Salack, S., Giannini, A., Diakhate, M., Gaye, A., and Muller, B.: Oceanic influence on the sub-seasonal to interannual timing and frequency of extreme dry spells over the West African Sahel, Climate Dynamics, 42, https://doi.org/10.1007/s00382-013-1673-4, 2013.

Salack, S., Klein, C., Giannini, A., Sarr, B., Worou, N., Belko, N., Bliefernicht, J., and Kunstman, H.: Global warming induced hybrid rainy seasons in the Sahel, Environmental Research Letters, 11, 104 008, https://doi.org/10.1088/1748-9326/11/10/104008, 2016.

Sane, Y., Panthou, G., Bodian, A., Vischel, T., Lebel, T., Dacosta, H., Quantin, G., Wilcox, C., Ndiaye, O., Diongue Niang, A., and Diop Kane, M.: Intensity-Duration-Frequency (IDF) rainfall curves in Senegal, Natural Hazards and Earth System Sciences Discussions, 18, 1–30, https://doi.org/10.5194/nhess-18-1849-2018, 2018.

Sarr, B.: Present and future climate change in the semi-arid region of West Africa: A crucial input for practical adaptation in agriculture, Atmospheric Science Letters, 13, 108–112, https://doi.org/10.1002/asl.368, 2012.

Seck, A.: Le «Heug» ou pluie de saison sèche au Sénégal, https://doi.org/10.3406/geo.1962.16196, https://www.persee.fr/doc/geo_0003-4010_1962_num_71_385_16196, 1962.

Shuhong, W., Liu, J., Wang, J., Qiao, X., and Zhang, J.: Evaluation of GPM IMERG V05B and TRMM 3B42V7 Precipitation Products over High Mountainous Tributaries in Lhasa with Dense Rain Gauges, Remote Sensing, 11, 20, https://doi.org/10.3390/rs11182080, 2019.

Siegmund, J., Bliefernicht, J., Laux, P., and Kunstmann, H.: Toward a Seasonal Precipitation Prediction System for West Africa: Performance of CFSv2 and High Resolution Dynamical Downscaling, Journal of Geophysical Research: Atmospheres, 120, n/a–n/a, https://doi.org/10.1002/2014JD022692, 2015.

Sivakumar, M.: Empirical analysis of dry spells for agricultural applications in west Africa, Journal of Climate, 24, 532–539, 1992.

Tabios, G. and Salas, J.: A Comparative Analysis of Techniques for Spatial Interpolation of Precipitation, Journal of the American Water Resources Association, 21, 365–380, https://doi.org/doi.org/10.1111/j.1752-1688.1985.tb00147.x, 1985.

Taylor, C., Belušić, D., Guichard, F., Parker, D., Vischel, T., Bock, O., P. Harris, P., Janicot, S., Klein, C., and Panthou, G.: Frequency of extreme Sahelian storms tripled since 1982 in satellite observations, Nature, 544, 475–478, https://doi.org/10.1038/nature22069, 2017.

Taylor, K. E.: Summarizing multiple aspects of model performance in a single diagram, Journal of Geophysical Research, 106, 7183–7192, https://doi.org/10.1029/2000JD900719, 2001.

Thorne, V., Coakeley, P., Grimes, D., and Dugdale, G.: Comparison of TAMSAT and CPC Rainfall Estimates with rainfall, for southern Africa, International Journal of Remote Sensing, 22, 1951–1974, https://doi.org/10.1080/01431160118816, 2001.

Thuo, M., Bravo-Ureta, B., Obeng-Asiedu, K., and Hathie, I.: The Adoption of Agricultural Inputs by Smallholder Farmers: The Case of an Improved Groundnut Seed and Chemical Fertilizer in the Senegalese Groundnut Basin, Journal Of Developing Areas, 48, pp. 61–82, https://doi.org/10.1353/jda.2014.0014, 2014.

Tian, Y., Peters-Lidard, C., Choudhury, B., and Garcia, M.: Multi-Temporal Analysis of TRMM-Based Satellite Precipitation Products for Land Data Assimilation Applications, Journal of Hydrometeorology, 8, https://doi.org/10.1175/2007JHM859.1, 2007.

Trenberth, K. E.: Attribution of Climate Variations and Trends to Human Influences and Natural Variability, Wiley Interdisciplinary Reviews: Climate Change, 2, 925 – 930, https://doi.org/10.1002/wcc.142, 2011.

Trenberth, K. E., Dai, A., M. Rasmussen, R., and Parsons, D.: The Changing Character of Precipitation, Bull. Amer. Meteor. Soc., 84, 1205–1217, https://doi.org/10.1175/BAMS-84-9-1205, 2003.

Washington, R., Harrison, M., Conway, D., Black, E., Challinor, A., Grimes, D., Jones, R., Morse, A., Kay, G., and Todd, M.: African Climate Change: Taking the Shorter Route, Bulletin of the American Meteorological Society, 87, https://doi.org/10.1175/BAMS-87-10-1355, 2006.

Wei, C., Chiang, J.-L., Wey, T. H., Yeh, H., and Cheng, Y.: Rainfall Network Design using Entropy and Kriging Approach, 11, 4927, 2009.

WFP: WFP Senegal Country Brief, January 2018, 2018.

Wilcox, C., Vischel, T., Panthou, G., Bodian, A., Blanchet, J., Descroix, L., Quantin, G., Cassé, C., Tanimoun, B., and Kone, S.: Trends in hydrological extremes in the Senegal and Niger Rivers, Journal of Hydrology, 566, https://doi.org/10.1016/j.jhydrol.2018.07.063, 2018.

Xie, P., Joyce, R., Wu, S., Yoo, S.-H., Yarosh, Y., Sun, F., and Lin, R.: Reprocessed, Bias-Corrected CMORPH Global High-Resolution Precipitation Estimates from 1998, Journal of Hydrometeorology, 18, https://doi.org/10.1175/JHM-D-16-0168.1, 2017.

Xu, F., Guo, B., Ye, B., Ye, Q., Chen, H., Ju, X., Jinyun, G., and Wang, Z.: Systematical Evaluation of GPM IMERG and TRMM 3B42V7 Precipitation Products in the Huang-Huai-Hai Plain, China, Remote Sensing, 11, 697, https://doi.org/10.3390/rs11060697, 2019.

Yeni, F. and Alpas, H.: Vulnerability of global food production to extreme climatic events, Food Research International, 96, https://doi.org/10.1016/j.foodres.2017.03.020, 2017.

Zeweldi, D. and Gebremichael, M.: Evaluation of CMORPH Precipitation Products at Fine Space-Time Scales, Journal of Hydrometeorology - J HYDROMETEOROL, 10, https://doi.org/10.1175/2008JHM1041.1, 2009.

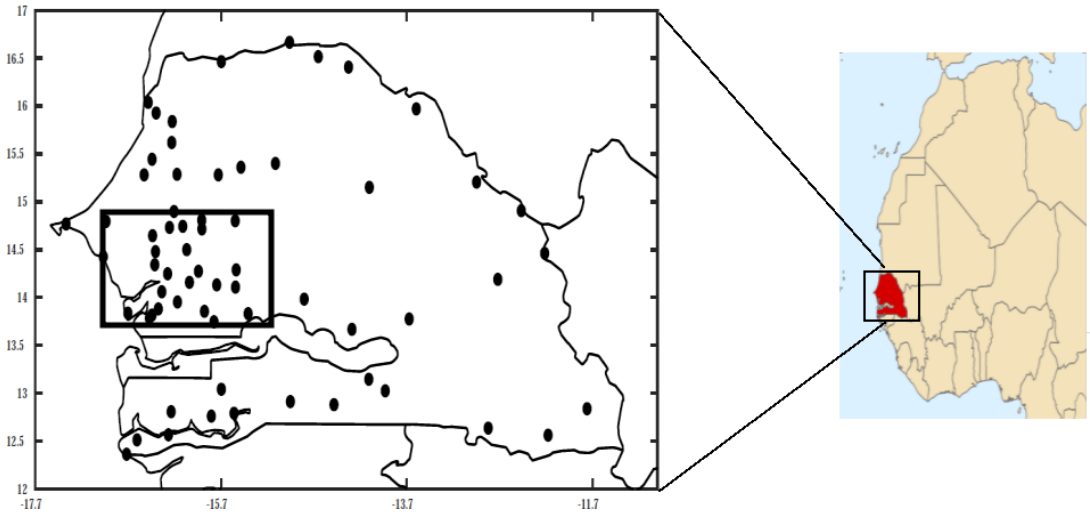

Figure 1. Map of Senegal and West Africa (inset). The black dots indicate the location of the 65 ANACIM raingauges used for this study. The square in central western of Senegal illustrates the location of the groundnut basin (area of high density of raingauges).

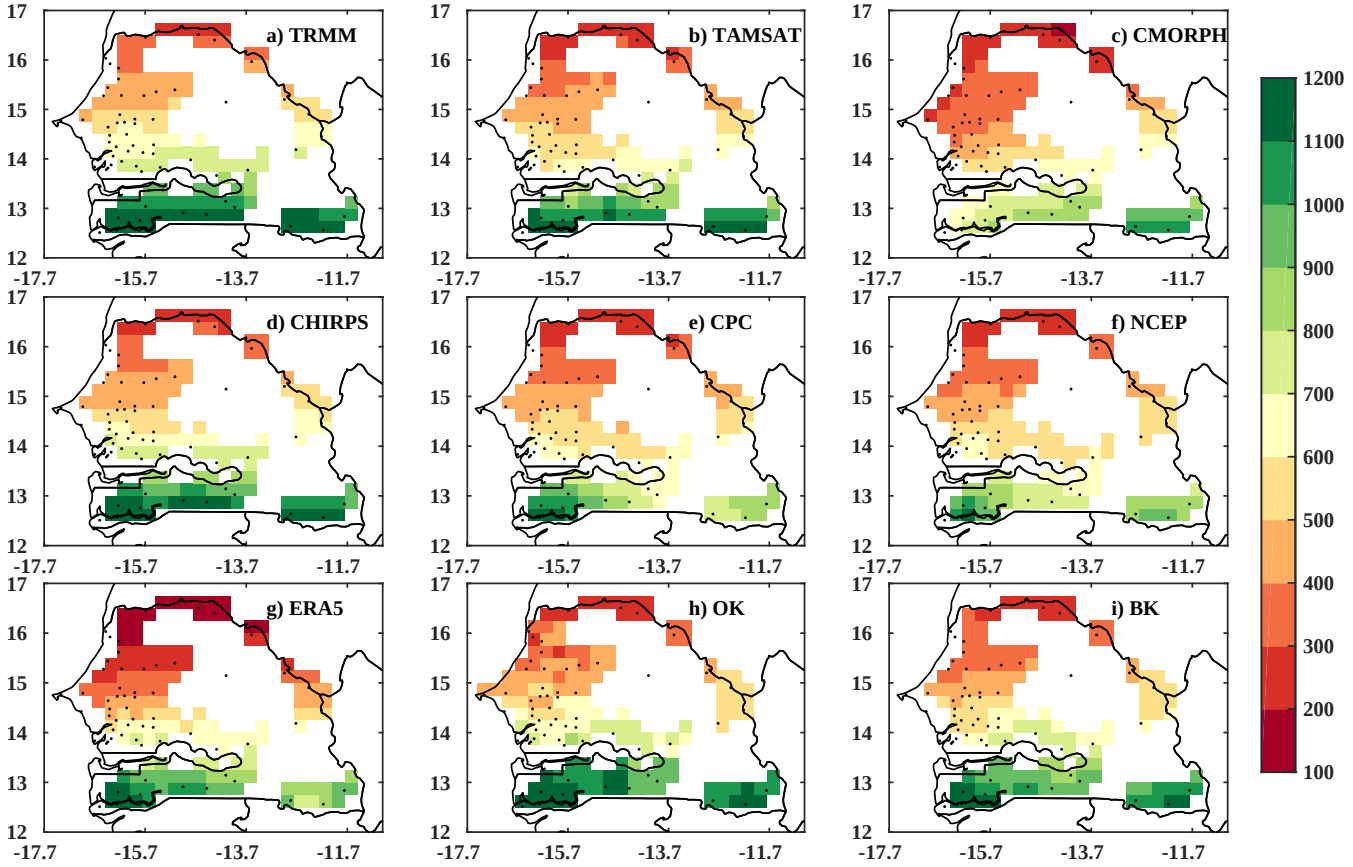

Figure 2. Spatial distribution of average seasonal rainfall from June to October over the overlap period between datasets (1998-2010, in mm): using a) TRMM b) TAMSAT c) CMORPH d) CHIRPS, e) CPC, f) NCEP g) ERA5 h) OK i) BK. The black dots represent the stations used. Details of the datasets are provided in Table 1

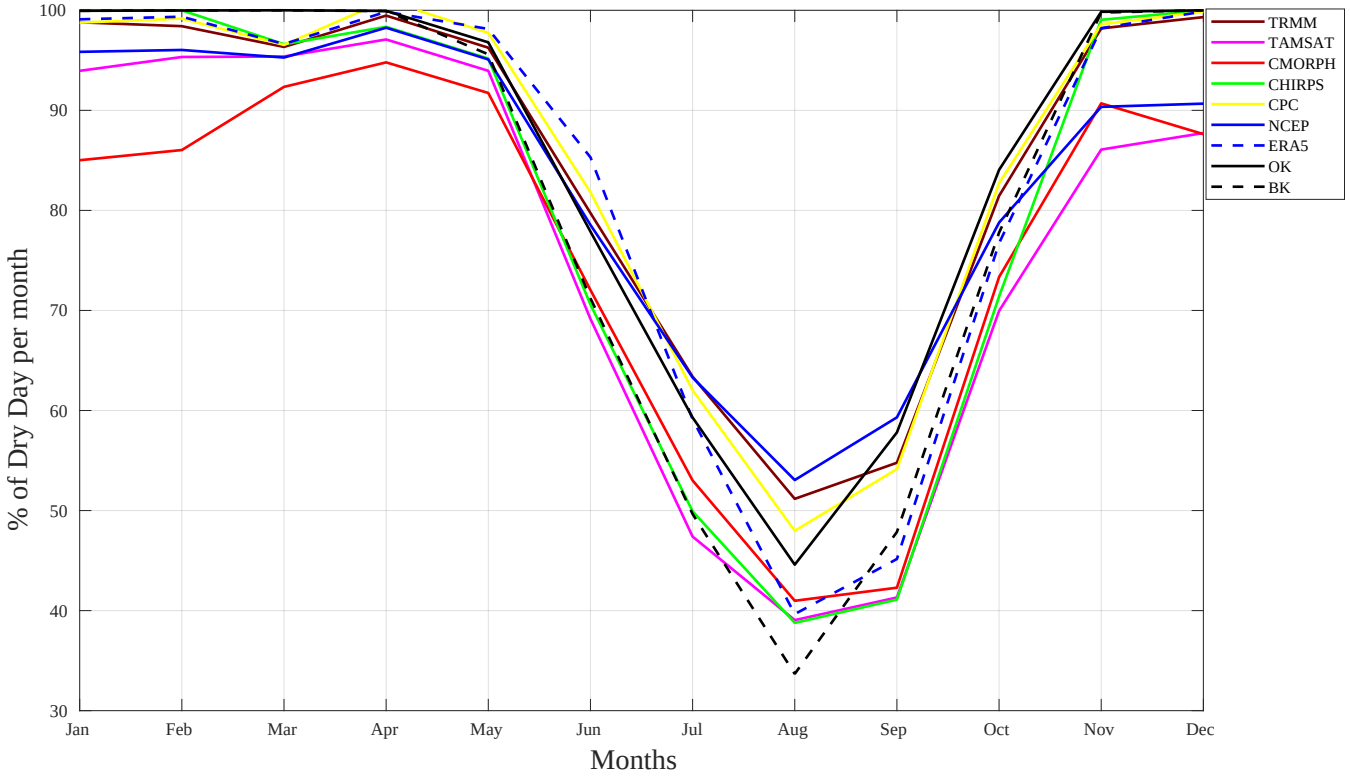

Figure 3. Percentage of average dry day (<= 1 mm) per month computed over the overlap period between datasets (1998-2010) and over all grid points in each datasets : TRMM, TAMSAT, CMORPH, CHIRPS, CPC, NCEP, ERA5, BK, OK

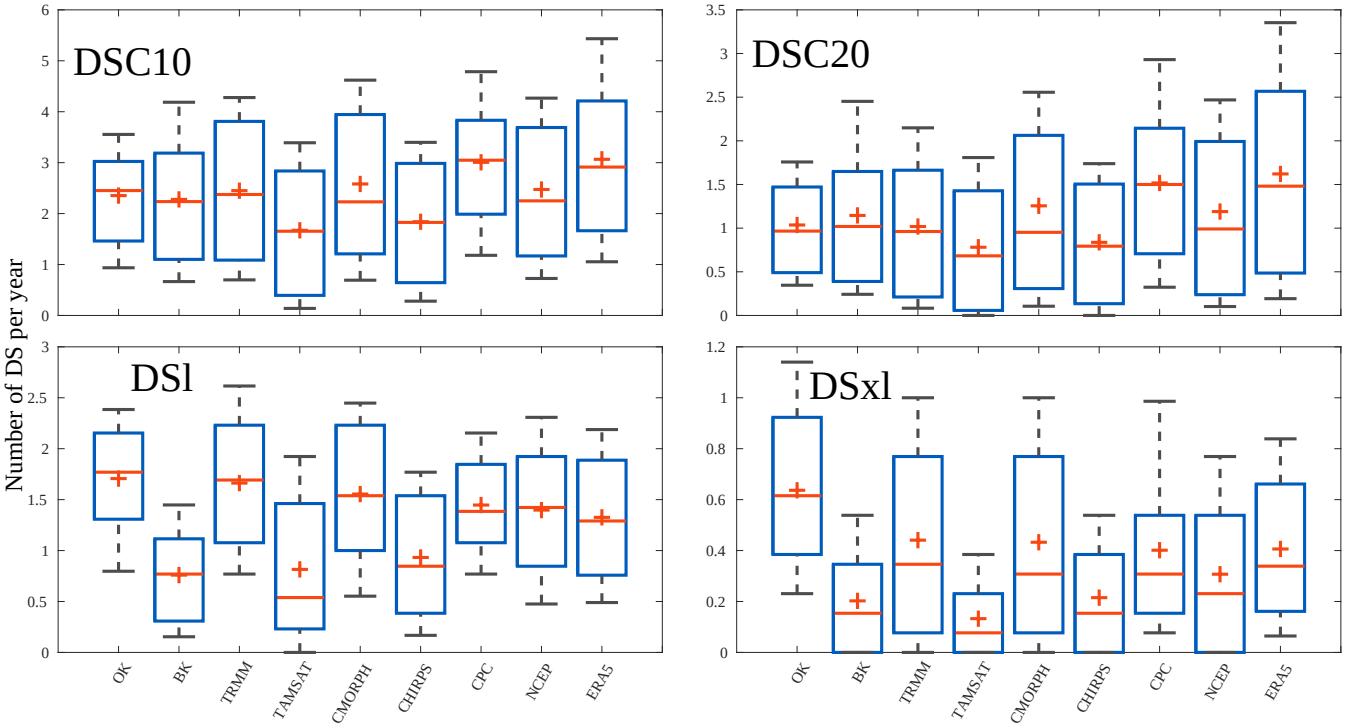

Figure 4. Boxplots of average number of dry spells (DSC10, DSC20, DSl and DSxl) per year collected on all grid points for the 9 gridded datasets used (TRMM, TAMSAT, CMORPH, CHIRPS, CPC, NCEP, ERA5, BK, OK). The $-$ represent the median value, The $+$ represent the mean value, the left and right edges of the box represent the 25th and 75th percentile values, respectively, while the "whiskers" represent the extreme values. The average number of dry spells is computed on the overlap period (1998-2010). Details on the datasets and dry spells are provided in Tables 1 and 2 , respectively.

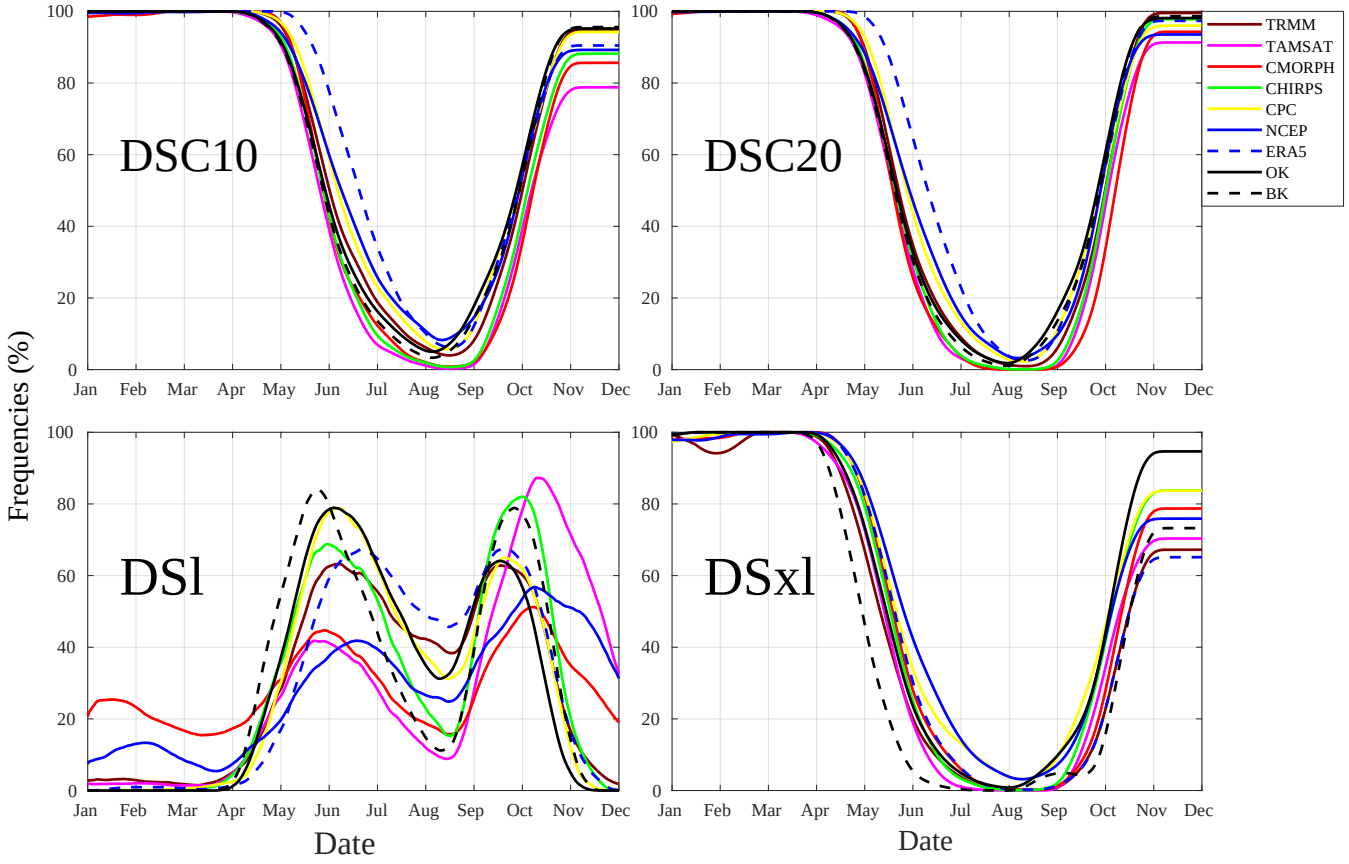

Figure 5. Seasonal cycle of four categories of dry spells (DSC10, DSC20, DSl and DSxl) used in this study computed over the overlap between datasets (1998-2010) : TRMM, TAMSAT, CMORPH, CHIRPS, CPC, NCEP, ERA5, BK, OK. Details on the datasets and dry spells are provided in Tables 1 and 2 , respectively

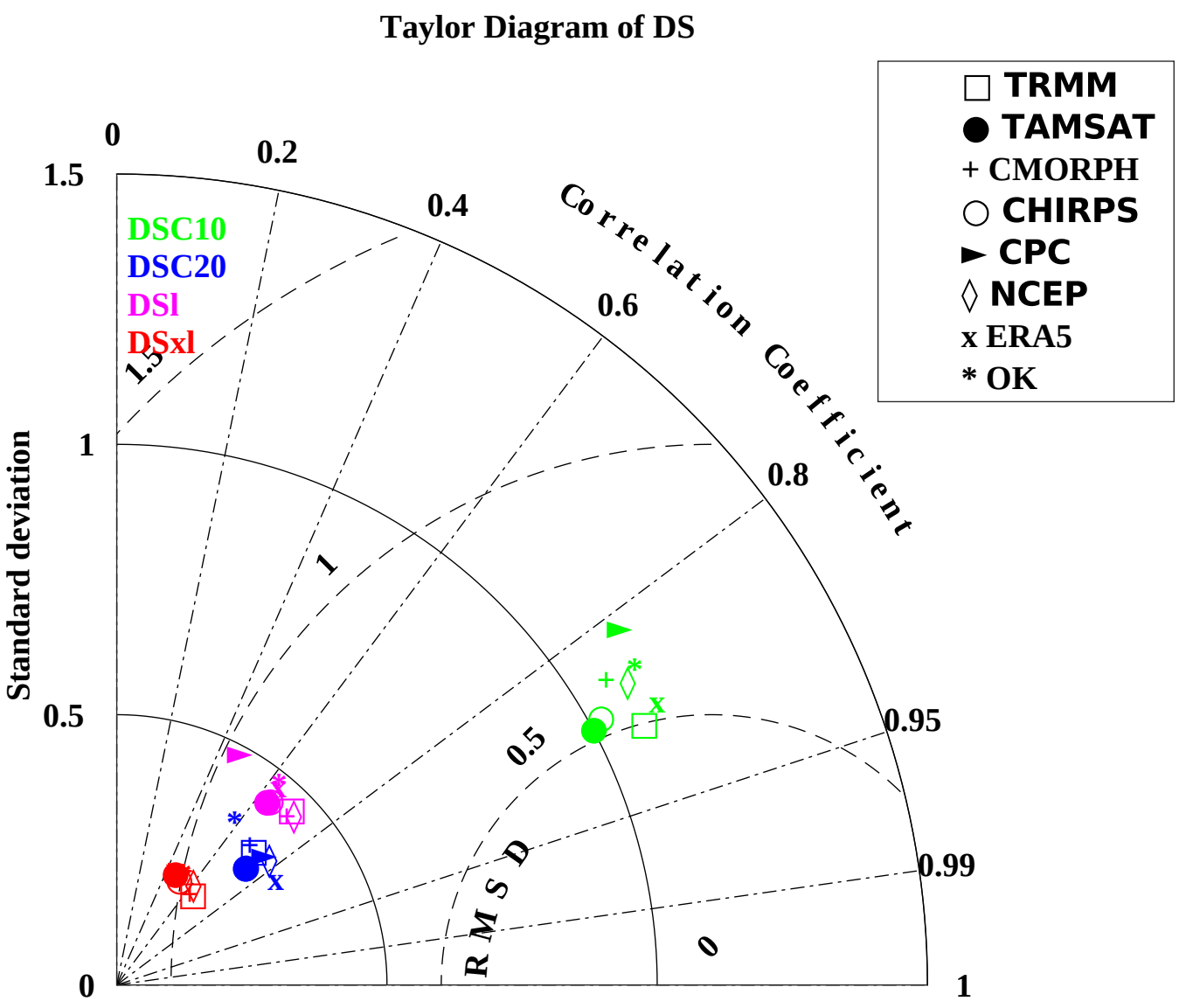

Figure 6. Taylor diagram providing 3 statistical scores (standard deviation, Correlation coeficient, root mean square deviation) with Radius expresses the standard deviation, the angle the correlation and the distance from the bottom right point the RMSD, OK dataset is considered as a reference to compare the spatial distribution of the four categories of dry spells (DSC10, DSC20, DSl and DSxl) of the different datasets: TRMM, TAMSAT, CMORPH, CHIRPS, CPC, NCEP, ERA5, BK. Details on the datasets and dry spells are provided in Tables 1 and 2 , respectively

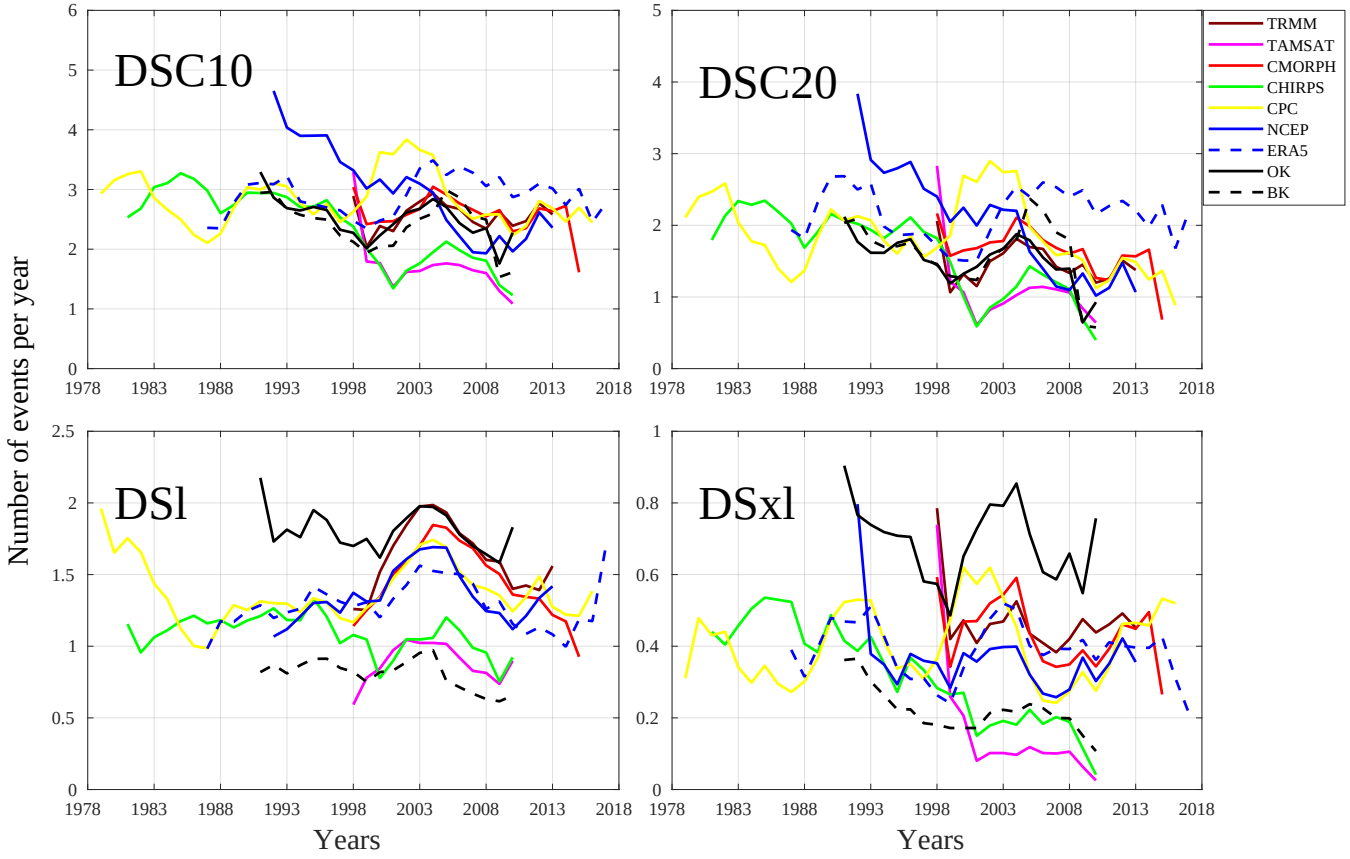

Figure 7. Interannual variability of the average number on all grid points of DSC10, DSC20, DSl and DSxl computed over the period at our availability for each datasets: TRMM (1998-2013), TAMSAT(1998-2010), CMORPH (1998-2015), CHIRPS (1981-2010), CPC (1979-2016), NCEP (1992-2013), ERA5 (1987-2017), BK (1991-2010), OK (1991-2010). Details on the datasets and dry spells are provided in Tables 1 and 2 , respectively

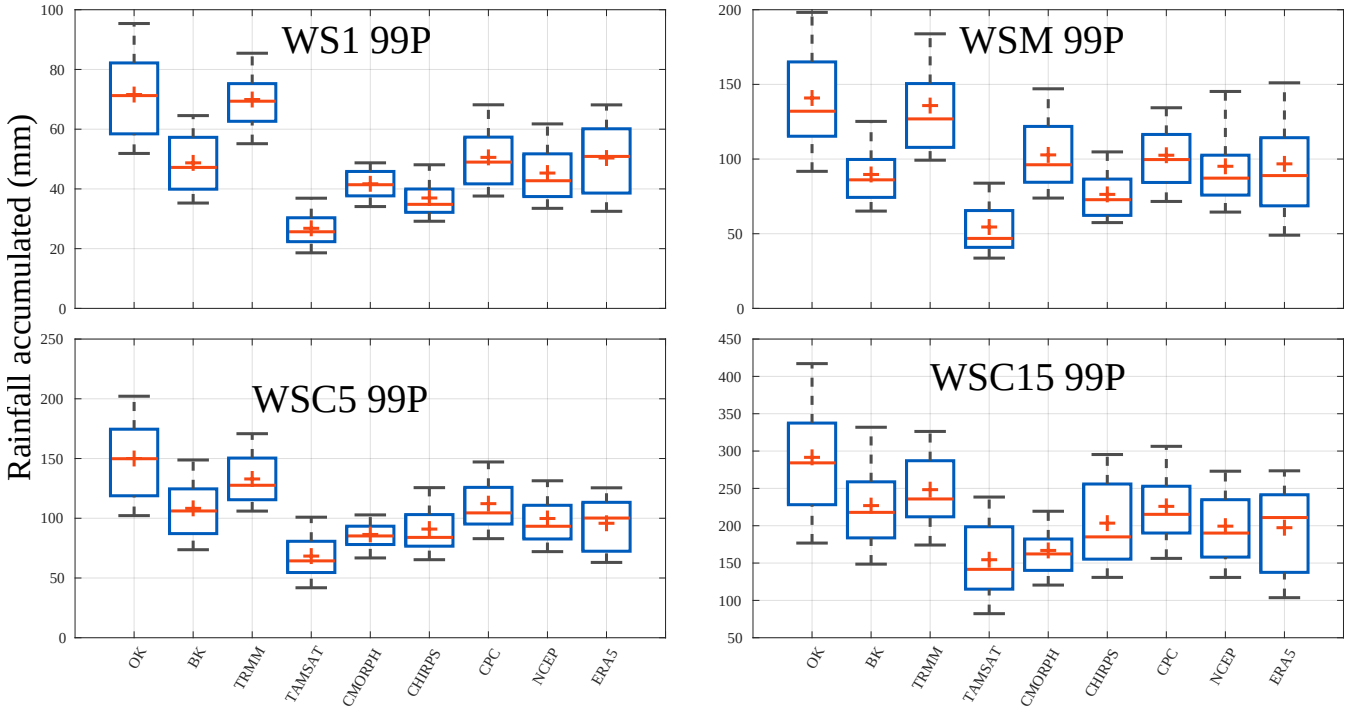

Figure 8. Boxplots of seasonal average amounts over all grids points from wet spells WS1, WSM, WSC5 and WSC15 (99^{th}) per year collected on all grid points for the 9 gridded datasets used (TRMM, TAMSAT, CMORPH, CHIRPS, CPC, NCEP, ERA5, BK, OK). The $-$ represent the median value, The $+$ represent the mean value, the left and right edges of the box represent the 25th and 75th percentile values, respectively, while the "whiskers" represent the extreme values. The average number of dry spells is computed on the overlap period (1998-2010). Details on the datasets and wet spells are provided in Tables 1 and 3 , respectively.

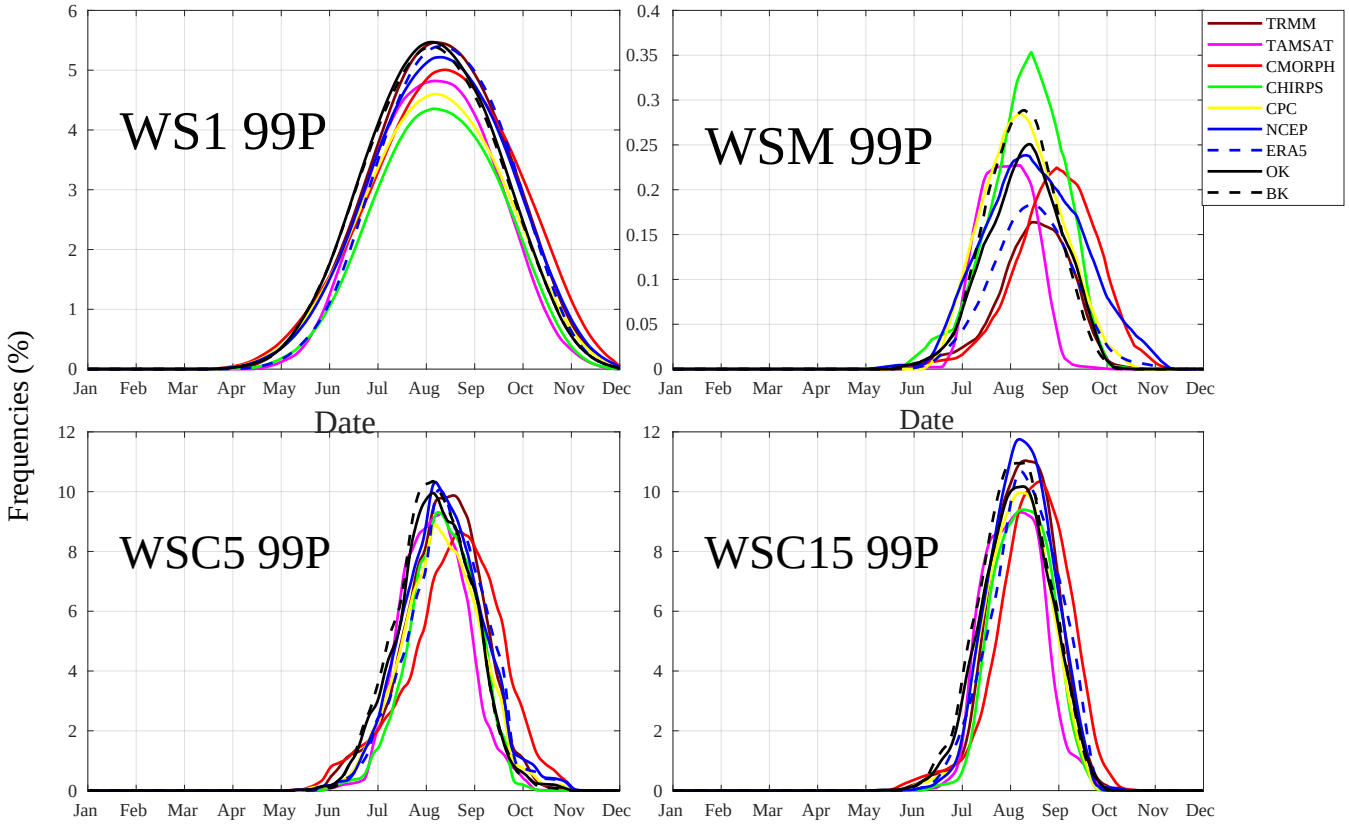

Figure 9. Seasonal cycle of four categories of wet spells WS1, WSM, WSC5 and WSC15 (99^{th}) used in this study computed over the overlap between datasets (1998-2010) : TRMM, TAMSAT, CMORPH, CHIRPS, CPC, NCEP, ERA5, BK, OK. Details on the datasets and wet spells are provided in Tables 1 and 3 , respectively

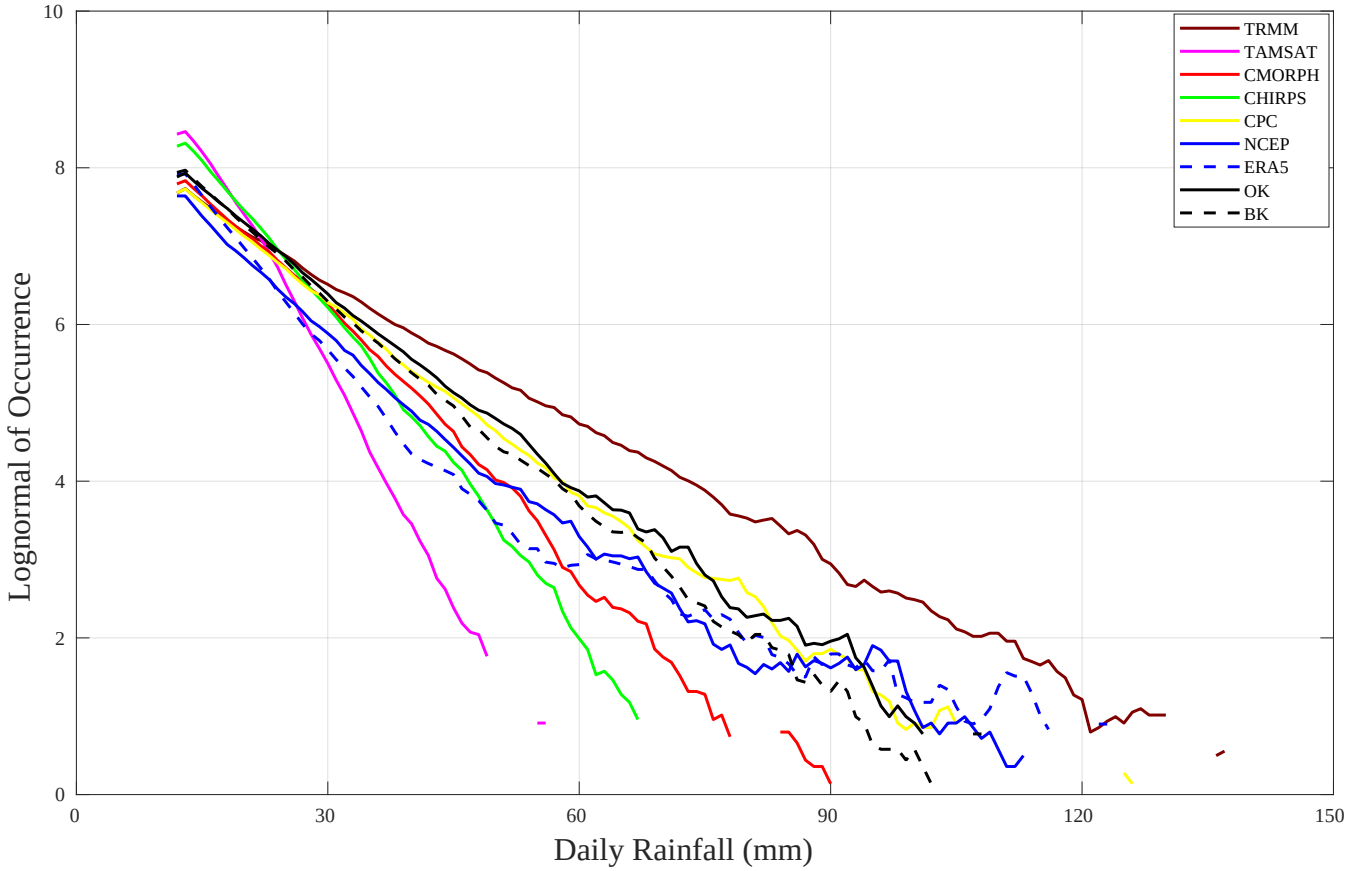

Figure 10. Comparison of the logarithmic distribution of daily rainfall amounts recorded at each grid point over the common period between datasets (1998-2010): TRMM, TAMSAT, CMORPH, CHIRPS, CPC, NCEP, ERA5, BK, OK on Senegal. Details of the datasets are provided in Table 1

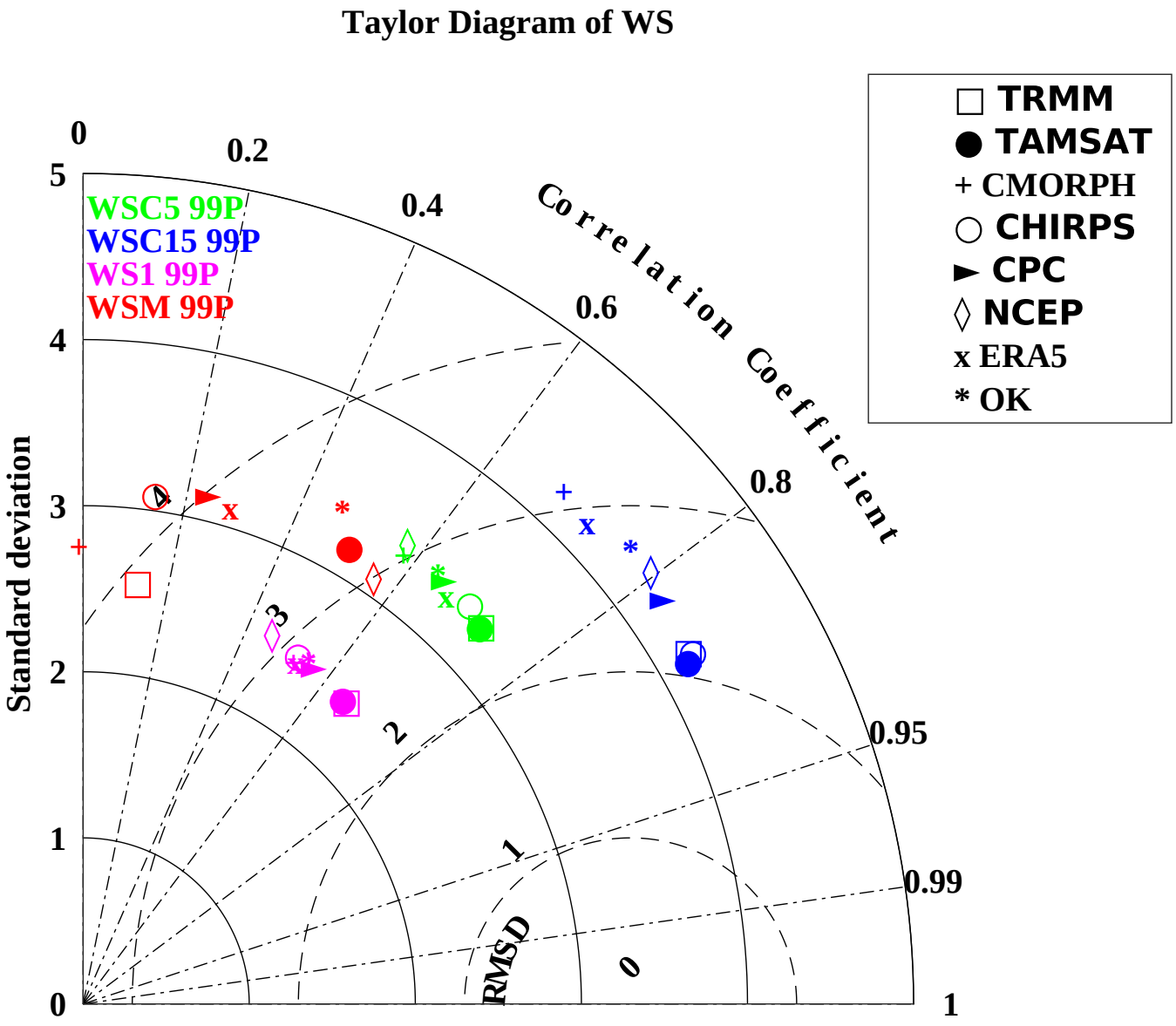

Figure 11. Taylor diagram providing 3 statistical scores (standard deviation, Correlation coeficient, root mean square deviation) with Radius expresses the standard deviation, the angle the correlation and the distance from the bottom right point the RMSD, OK dataset is considered as a reference to compare the spatial distribution of the four categories of wet spells WS1, WSM, WSC5 and WSC15 (99^{th}) of the different datasets: TRMM, TAMSAT, CMORPH, CHIRPS, CPC, NCEP, ERA5, BK. Details on the datasets and wet spells are provided in Tables 1 and 3 , respectively

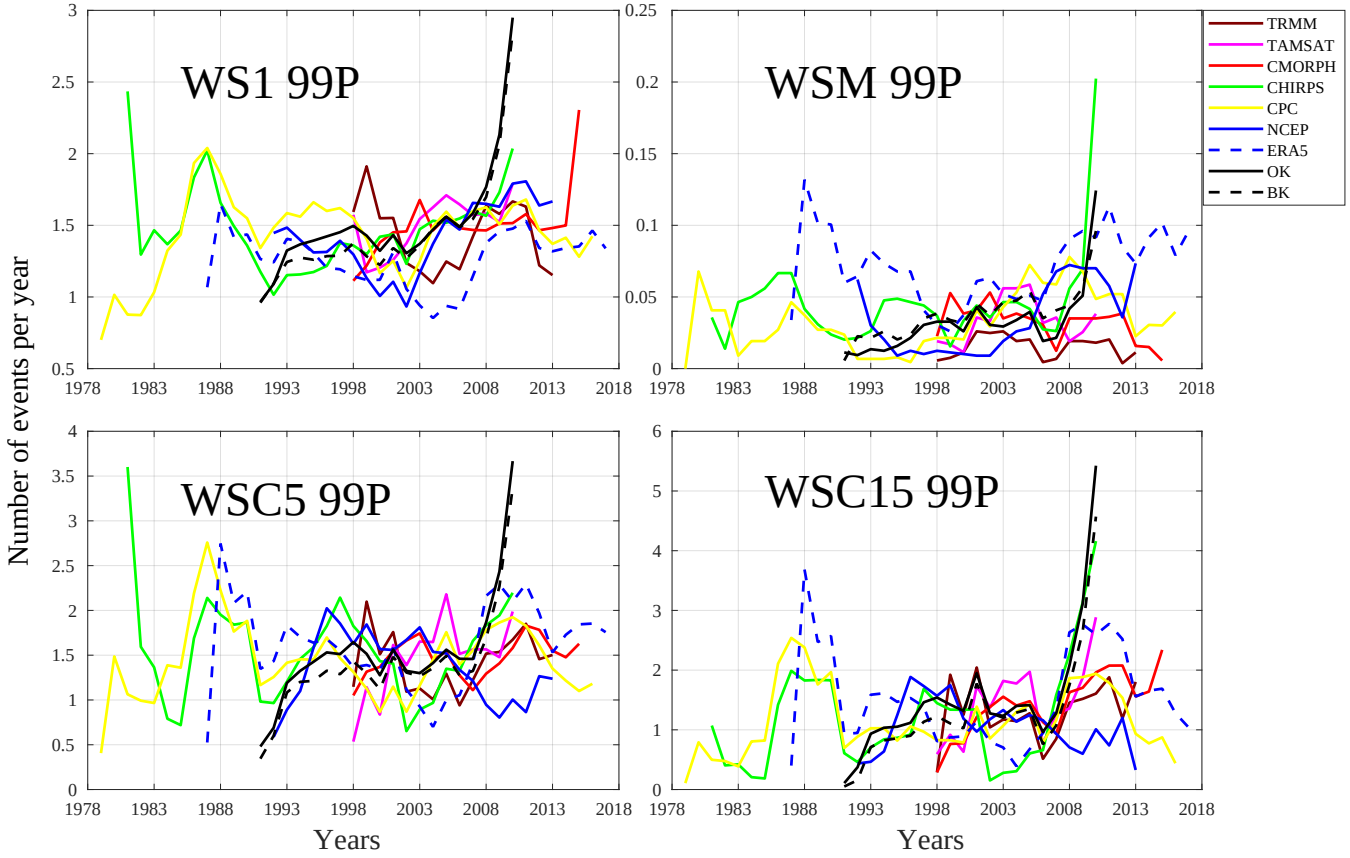

Figure 12. Interannual variability of the average number on all grid points of WS1, WSM, WSC5 and WSC15 (99^{th}) computed over the period at our availability for each datasets: TRMM (1998-2013), TAMSAT(1998-2010), CMORPH (1998-2015), CHIRPS (1981-2010), CPC (1979-2016), NCEP (1992-2013), ERA5 (1987-2017), BK (1991-2010), OK (1991-2010). Details on the datasets and wet spells are provided in Tables 1 and 3 , respectively

Table 1. Summary of the 9 datasets used in this study. The abbreviations in the data sources column are defined as follows: S, satellite; R, reanalysis; G, raingauge.

Name	Details	Data Sources	Spatial Resolution	Temporal Resolution	Temporal Coverage
TRMM 3B42 (V7)	Tropical Rainfall Measuring Mission (TRMM) 3B42 (V7)	S	$0.25^o \times 0.25^o$	$3-hourly$	1998 - $present$
CMORPH V1.0	CPC MORPHing technique (CMORPH) V1.0	S	$0.05^o \times 0.05^o$	$30min$	1998 - $present$
CHIRPS V2.0	Climate Hazards group InfraRed Precipitation (CHIRP) V2.0	S, R, G	$0.05^o \times 0.05^o$	$Daily$	1981 - $present$
TAMSAT V3	Tropical Applications of Meteorology using satellite data and ground based observations V3	S, G	$0.0375^o \times 0.0375^o$	$Daily$	1983 - $present$
NCEP-CFSR	National Centers (CFSR) for Environmental Prediction (NCEP) Climate Forecast System Reanalysis	R	$0.31^o \times 0.31^o$	$Hourly$	1979 - 2010
ERA5	European Centre for Medium range Weather Forecasts ReAnalysis 5 (ERA5)	R	$0.1^o \times 0.1^o$ Native resolution is 9 km	$Hourly$	1987 - $present$
CPC Unified V1.0/RT)	CPC Unified Gauge-based Analysis of Global Daily Precipitation V1.0/RT	G	$0.5^o \times 0.5^o$	$Daily$	1979 - $present$
OK	Ordinary Kriging	G	$0.25^o \times 0.25^o$	$Daily$	1991 - 2010
BK	Block Kriging	G	$0.25^o \times 0.25^o$	$Daily$	1991 - 2010

Table 2. Definition of indices to detect the Dry Spells

Dry Spells Indices	Definitions
DSC5	5 days with less than 5 mm of rainfall
DSC10	10 days with less than 10 mm of rainfall
DSC15	15 days with less than 15 mm of rainfall
DSC20	20 days with less than 20 mm of rainfall
DSs	1-3 consecutive dry days
DSm	4-7 consecutive dry days
DSl	8-14 consecutive dry days
DSxl	consecutive dry days exceding 15 days

Table 3. Definition of indices to detect the Wet Spells, XX for 90, 95, 99 and 99.5 percentiles

Wet Spells Indices	Definitions
WS1 *XX*P	1day with rainfall $> XX^{th}$p of daily rainfall
WSM *XX*P	2 day or more with rainfall $> XX^{th}$p of daily rainfall
WSC5 *XX*P	5-d precip. $> XX^{th}$p of 5-day cumulative rainfall
WSC10 *XX*P	10-d precip. $> XX^{th}$p of 10-day cumulative rainfall
WSC15 *XX*P	15-d precip. $> XX^{th}$p of 15-day cumulative rainfall
WSC20 *XX*P	20-d precip. $> XX^{th}$p of 20-day cumulative rainfall